MOLECULAR AND CELLULAR BIOLOGY, Jan. 2009, p. 129–139 Vol. 29, No. 1
0270-7306/09/$08.00+0 doi:10.1128/MCB.00963-08

Novel Proteolytic Processing of the Ectodomain of the Zinc Transporter ZIP4 (SLC39A4) during Zinc Deficiency Is Inhibited by Acrodermatitis Enteropathica Mutations▽

Taiho Kambe† and Glen K. Andrews*

Department of Biochemistry and Molecular Biology, University of Kansas Medical Center, Kansas City, Kansas 66160-7421

Received 18 June 2008/Returned for modification 18 July 2008/Accepted 14 October 2008

The zinc transporter ZIP4 (SLC39A4) is mutated in humans with the rare, autosomal recessive genetic disease acrodermatitis enteropathica. In mice, this gene is essential during early embryonic development. ZIP4 is dynamically regulated by multiple posttranscriptional mechanisms, and studies of mouse ZIP4 reported herein reveal that the ectodomain, the extracellular amino-terminal half of the protein, is proteolytically removed during prolonged zinc deficiency while the remaining eight-transmembrane carboxyl-terminal half of the protein is accumulated on the plasma membrane as an abundant form of ZIP4. This novel ZIP4 processing occurs in vivo in the intestine and visceral endoderm, in mouse Hepa cells that express the endogenous *Slc39a4* gene and in transfected MDCK and CaCo2 cells, but not HEK293 cells. In transfected MDCK and CaCo2 cells, the ectodomain accumulated and remained associated with membranes when zinc was deficient. ZIP4 cleavage was attenuated by inhibitors of endocytosis, which suggests that the processed protein is recycled back to the plasma membrane and that the ectodomain may be internalized. Ectodomain cleavage is inhibited by acrodermatitis enteropathica mutations near a predicted metalloproteinase cleavage site which is also essential for proper ectodomain cleavage, and overexpression of processed ZIP4 or ZIP4 with ectodomain truncations rendered the mouse *Mt1* gene hypersensitive to zinc. These finding suggest that the processing of ZIP4 may represent a significant regulatory mechanism controlling its function.

Zinc deficiency during pregnancy impairs embryonic, fetal, and postnatal development, leading to growth retardation, abnormal morphogenesis, immune system dysfunction, skin lesions, and neurological disorders in mammals (reviewed in references 8 and 22). Therefore, the ability to acquire zinc from the diet via the intestine and transfer it to the embryonic environment via the visceral yolk sac ([VYS] in mice) plays a critical role in the growth and morphogenesis of the embryo and subsequent health status of offspring. The zinc transporter SLC39A4 (ZIP4) is an essential component for the acquisition of zinc. Mutations in the human *SLC39A4* gene cause a rare autosomal recessive genetic disorder of zinc deficiency called acrodermatitis enteropathica (AE) (10, 32); in mice the *Slc39a4* gene is essential during early embryogenesis, and homozygous embryos die soon after implantation (5). Furthermore, heterozygous *Slc39a4* knockout mice are significantly underrepresented after birth and are hypersensitive to dietary zinc deficiency (5).

Recent studies reveal that the expression of *Slc39a4* is regulated at multiple posttranscriptional levels in response to changes in zinc availability (2, 9, 15, 33). For example, during zinc deficiency this mRNA is stabilized, leading to increased accumulation of *Slc39a4* mRNA and ZIP4 protein and the localization of ZIP4 at the apical surfaces of enterocytes and visceral endoderm cells (4, 33). In contrast, repletion of zinc to normal levels causes the rapid endocytosis and degradation of ZIP4 and destabilization of *Slc39a4* mRNA (33). Similar results were obtained with in vitro transfection studies of recombinant ZIP4, which demonstrated that ZIP4 was degraded via a process that requires both the proteasomal and lysosomal compartments (9, 15). Thus, dynamic posttranscriptional control of ZIP4 in response to zinc plays an important role in regulating zinc homeostasis.

Previous studies from our laboratory revealed that during prolonged zinc deficiency, apparently full-length ZIP4 and its glycosylated forms (~75 kDa and larger) are detectable in membrane preparations from the intestine and VYS, but by far the major immunoreactive ZIP4 peptide detected by Western blotting was ~37 kDa in apparent molecular mass, or about half the predicted size of full-length ZIP4 (2, 7, 33). This observation was explored further herein, and our results demonstrate that the ~37-kDa peptide represents ZIP4 lacking the N-terminal extracellular domain or ectodomain. This novel processing of ZIP4 occurs in response to zinc deficiency in polarized epithelial cells like MDCK and CaCo2 as well as in mouse Hepa cells, mimicking the results obtained in mice. The evidence suggests that the ectodomain of ZIP4 accumulates as a peripheral membrane protein, whereas the remainder of the processed protein is apparently recycled back to the apical membrane. Overexpression of processed ZIP4 or ZIP4 with ectodomain truncations correlated with hypersensitivity to zinc, as shown by a dramatic reduction in the dose response for induction of *Mt1* (metallothionein 1) gene expression. Furthermore, AE mutations near the predicted cleavage site of the ectodomain block processing of ZIP4. Thus, this novel regulation of ZIP4 may be an additional and important regulatory

* Corresponding author. Mailing address: Department of Biochemistry and Molecular Biology, Mail Stop 3030, University of Kansas Medical Center, 39th and Rainbow Blvd., Kansas City, KS 66160-7421. Phone: (913) 588-6935. Fax: (913) 588-3920. E-mail: gandrews@kumc.edu.

† Permanent address: Division of Integrated Life Science, Graduate School of Biostudies, Kyoto University, Kyoto 606-8502, Japan.

▽ Published ahead of print on 20 October 2008.

mechanism controlling zinc transport or other activities of this critical zinc transporter.

MATERIALS AND METHODS

Cell culture. Mouse Hepa cells and HEK293 and CaCo2 cells were maintained at 37°C in a humidified 5% CO_2 incubator in Dulbecco's modified Eagle medium (DMEM) containing 10% fetal bovine serum (FBS), 100 units of penicillin/ml, and 100 μg of streptomycin/ml. MDCK cells were cultured in DMEM/F-12 medium containing 5% FBS. To generate zinc-deficient culture medium, FBS was treated with Chelex-100 resin (18). The sodium form of Chelex-100 (200 to 400 mesh) (Bio-Rad) was adjusted to neutral pH and incubated (100 g/500 ml) with FBS for 1 h at room temperature, according to the manufacturer's instructions. Chelex-treated FBS was filter sterilized, aliquoted, and stored at −80°C. Metal concentrations were measured by inductively coupled plasma mass spectrometry (7, 21). DMEM or DMEM/F-12 was adjusted to 10% or 5%, respectively, with Chelex-treated FBS, which restored all the essential metals to near normal concentrations except for zinc, which was reduced about 100-fold. Where indicated on Fig. 2 and 4, cells were cultured for at least 4 days on 24-mm polyester membrane Transwell plates with 0.4-μm pores (Costar) to allow the formation of tight junctions.

Expression vector construction. A Zip4-hemagglutinin (HA) expression vector encoding mouse ZIP4 with an HA tag at the carboxyl terminus was described previously (9, 31). This vector was modified by inserting a FLAG tag (DYKDD DDK) preceding codon N26 to generate the FLAG-ZIP4-HA expression vector. Other point mutations were introduced into the mouse ZIP4-HA expression vector using a two-step PCR method, as described previously (13, 25). Mutations were confirmed by DNA sequencing of both strands and are presented in the cartoon in Fig. 5A and detailed in the legend to Fig. 5. The Δ337 mutant was constructed by deleting the coding sequence from amino acids 1 to 336 and fusing a leader peptide sequence encoding MEVLLGVKIGC to the new amino terminus using the two-step PCR method. The Δ287 mutant was constructed by deleting the sequence encoding amino acids 1 to 286 (between the BamHI-XcmI sites of ZIP4-HA), making M287 the start codon.

Transfection. Hepa, MDCK, HEK293, and CaCo2 cells were seeded (6×10^5 to 8×10^5 cells) in 60-cm dishes and transfected with ZIP4-HA, FLAG-ZIP4-HA, or mutated ZIP4-HA expression vectors as indicated in the figure legends. Transfections were performed using Lipofectamine reagent (Invitrogen) for Hepa cells and Lipofectamine 2000 (Invitrogen) for HEK293, MDCK, and CaCo2 cells. To create pools of stably transfected cells, cells were transfected with the above expression vectors and then selected in medium containing 5 to 10 μg/ml puromycin (Sigma) for 2 to 4 weeks. Surviving cells were pooled, and pools of HEK293, MDCK, and CaCo2 cells expressed ZIP4 in 80 to 90%, 40 to 50%, and 20 to 30% of the cells, respectively.

Cell surface biotinylation and detection of ZIP4. MDCK and CaCo2 cells were grown on transwell plates until polarized and then cultured in medium containing normal FBS or Chelex-treated FBS for 48 h. Before biotinylation, cells were washed twice with ice-cold phosphate-buffered saline (PBS) supplemented with 0.1 mM $CaCl_2$ and 1.0 mM $MgCl_2$, and then EZ-Link, a sulfo-NHS-SS-biotin [sulfosuccinimidyl 2-(biotinamido)-ethyl-1,3-dithiopropionate] reagent (Pierce), was added to the apical compartment or the basolateral compartment according to the manufacturer's instructions (Pierce). Cells were incubated with EZ-Link reagent for 30 min at 4°C, washed as above, and incubated again with EZ-Link reagent. After a quenching step with quenching solution (Pierce), the cells were washed twice with PBS, and the polyester membrane was excised from the transwell plate with a scalpel. The membrane was placed in a 1.5-ml microcentrifuge tube with 300 μl of NP-40 buffer (50 mM HEPES-HCl, pH 7.4, 100 mM NaCl, 1.5 mM $MgCl_2$, 1% Nonidet P-40, 0.5% deoxycholate, and 0.1% sodium dodecyl sulfate [SDS]) and sonicated for 20 s. The membrane was removed, and the sonicated cells were centrifuged at 10,000 × *g* for 5 min at 4°C. An aliquot (50 μl) of the supernatant was used to determine the input. Another aliquot (~250 μl) was precipitated with streptavidin-coupled Sepharose beads (Pierce). After the sample was washed with NP-40 buffer, biotinylated proteins were recovered from the streptavidin-coupled beads in 2× SDS sample buffer and then subjected to Western blot analysis.

Detection of cell surface ZIP4 protein using anti-FLAG and anti-HA antibodies. The presence of FLAG-ZIP4-HA on the plasma membrane was assessed by measuring the levels of anti-HA or anti-FLAG antibodies bound to the surface of fixed, nonpermeabilized Hepa cells, essentially as described previously (9). Hepa cells were transfected with the FLAG-ZIP4-HA expression vector in 12-well trays, washed twice with PBS on ice, and fixed with 4% paraformaldehyde. After two more washes with PBS, the cells were blocked with ice-cold 5% skim milk in PBS for 30 min and then incubated with anti-HA or anti-FLAG antibodies with gentle shaking for 1 h at room temperature. After the samples were washed extensively with PBS to remove unbound antibodies, cells were lysed by sonication in SDS lysis buffer. The solubilized anti-HA or anti-FLAG antibodies were then detected by Western blotting as described below. Both antibodies were detected using horseradish peroxidase-conjugated antibodies by chemiluminescence.

Preparation of membrane proteins and Western blot analysis. Mouse Hepa cells (~2×10^6) were collected by centrifugation, resuspended in 3 ml of ice-cold homogenization buffer (0.25 M sucrose, 20 mM HEPES, pH 7.4 and 1 mM EDTA containing protease inhibitors), and homogenized with 30 strokes of a tight-fitting 5-ml Dounce homogenizer. After removal of nuclei, the postnuclear supernatant was centrifuged for 15 min at 85,000 × *g* at 4°C. The membrane pellet was resuspended in NP-40 buffer. Na_2CO_3 extraction was performed as described previously (26). Briefly, membranes from stably transfected CaCo2 cells expressing FLAG-ZIP4-HA were resuspended in 0.1 M Na_2CO_3, pH 11.0, and incubated on ice for 30 min before centrifugation for 15 min at 85,000 × *g* at 4°C. The supernatant fraction (peripheral membrane proteins) and pellet fraction (integral membrane proteins) were recovered. Total cellular proteins from HEK293, MDCK, or CaCo2 cells were prepared by sonication of cells directly into NP-40 buffer, followed by centrifugation at 10,000 × *g* for 15 min at 4°C. Membrane proteins (20 μg) or total cellular proteins (20 μg) were resolved on 7.5% SDS-polyacrylamide gels and transferred to polyvinylidene difluoride membranes (33). Membranes were blocked for 1 h at room temperature and then incubated overnight at 4°C with primary antibody in blocking solution at these dilutions: ZIP4 antiserum, 1:600; ZIP1 antiserum, 1:800; ZnT5 (a zinc transporter) monoclonal antibody, 1:1,000; NaK-ATPase α1 subunit monoclonal antibody (Affinity BioReagents), 1:2,000; HA monoclonal antibody (HA.11; Covance), 1:3,000; and FLAG monoclonal antibody (M2; Sigma), 1:2,000. After extensive washing, membranes were incubated with goat anti-rabbit or anti-mouse horseradish peroxidase-conjugated secondary antibodies (Santa Cruz), and the blot was developed using ECL Plus reagent (Amersham Biosciences) according to the manufacturer's instructions and detected using Kodak BioMax MS film (Kodak).

RNA extraction and Northern blot hybridization. RNA was isolated using Trizol according to the manufacturer's instructions (Invitrogen). Total RNA (20 μg) was size fractionated by agarose-formaldehyde gel electrophoresis, transferred, and UV cross-linked to nylon membranes. Northern blot membranes were hybridized and washed under stringent conditions (3, 4). Hybrids were detected by autoradiography at −80°C. Duplicate gels were stained with acridine orange to ensure equivalent loading and integrity of total RNA. The probes for mouse *Slc39a4* and *Mt1* mRNAs were used at 2×10^6 cpm/ml of hybridization solution. The mouse *Mt1* probe crossed-hybridized with dog *Mt* mRNA and was therefore used to detect *Mt* mRNA in MDCK cells. Quantification of band intensities was performed on a Macintosh iBook G4 computer using the public domain NIH Image program (U.S. National Institutes of Health, http://rsb.info.nih.gov/nih-image).

RESULTS

When zinc is deficient, ZIP4 is synthesized and localizes to the apical surface of VYS endoderm cells (and intestine [not shown here]) in vivo and in plasma membrane in HEK293 cells (and in CaCo2 and MDCK cells [data not shown]) transfected with a ZIP4-HA expression vector in vitro (Fig. 1A), as previously published (2, 4, 9, 31, 33). Western blot analysis of ZIP4 (Fig. 1B) from the zinc-deficient VYS revealed bands corresponding to the predicted full-length (~75 kDa) ZIP4 and larger glycosylated forms of ZIP4, but by far the most intense band detected migrated as an ~37-kDa peptide. In the transfected HEK293 cells, only the predicted full-length ZIP4 band was detected regardless of zinc deficiency. In contrast, in transfected CaCo2 cells, zinc deficiency led to the formation of a major ~37-kDa band detected by an anti-HA antibody which recognizes the carboxyl-terminal HA tag on the expressed ZIP4 protein. The major ~37-kDa ZIP4 peptide from the zinc-deficient VYS cells and transfected CaCo2 cells comigrated during electrophoresis and was detected using an anti-peptide antibody directed against the large intracellular loop in

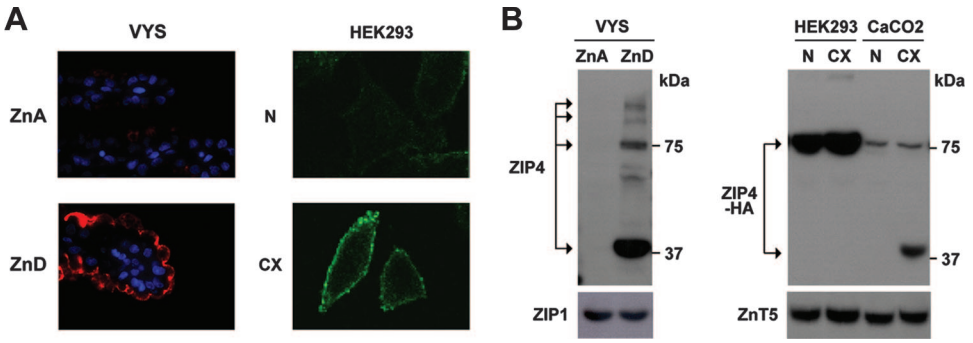

FIG. 1. ZIP4 is processed in the VYS and in transfected CaCo2 cells but not in transfected HEK293 cells during zinc deficiency. (A) Immunofluorescence localization of endogenous ZIP4 in the embryonic mouse VYS and in transfected HEK293 cells. Pregnant mice were fed a zinc-adequate diet (ZnA) or a zinc-deficient diet (ZnD) beginning on day 8 of pregnancy, and the VYS was recovered on day 14 and processed for detection of ZIP4 using an anti-peptide antibody directed against the large intracellular loop of ZIP4 (Fig. 5A). The methods employed and these results have been described in detail previously (2, 33). Red fluorescence indicates the localization of ZIP4, whereas nuclei are stained with DAPI (4′,6′-diamidino-2-phenylindole; blue). HEK293 cells were transfected with a mouse ZIP4-HA expression vector and cultured in medium containing either 10% normal FBS (N) or 10% Chelex-treated FBS (CX) for 48 h. Cells were processed for detection of ZIP4-HA without permeabilization using an anti-HA antibody. Green fluorescence indicates the localization of ZIP4-HA. (B) Western blot detection of ZIP4 in the ZnA and ZnD VYS and in transfected HEK293 and CaCo2 cells incubated in medium containing normal 10% FBS or Chelex-treated FBS. Membrane proteins were isolated and analyzed by Western blotting using an anti-peptide antibody against ZIP4 (VYS) or an anti-HA antibody (HEK293 and CaCo2). ZIP1 and ZnT5 are shown as loading controls.

ZIP4 in the VYS cells and/or the HA antibody directed against the extracellular carboxyl terminus in transfected cells (see cartoon in Fig. 5A). The size of this ~37-kDa ZIP4 peptide and its reactivity with these two antibodies suggest that it represents ZIP4 lacking the extracellular or ectodomain. We will refer to this peptide as processed ZIP4.

To further explore this observation, an expression vector for FLAG and HA double-tagged ZIP4 (FLAG-ZIP4-HA) was created in which the FLAG tag was inserted near the amino terminus of ZIP4 just past the predicted leader peptide, and the HA tag was at the carboxyl terminus (see cartoon in Fig. 5A). When FLAG-ZIP4-HA was transfected into HEK293 cells, only the ~75-kDa ZIP4 full-length peptide was detected using the anti-HA antibody or the anti-FLAG antibody, regardless of whether the culture medium was zinc deficient or whether cell density was low or high (Fig. 2 and 3A). In contrast, when FLAG-ZIP4-HA was expressed in MDCK cells, both the ~75-kDa and processed ZIP4 peptides were detected using the anti-HA antibody when zinc was replete, but the abundance of the processed ZIP4 peptide increased significantly when zinc was deficient in the culture medium. Similarly, when FLAG-ZIP4-HA was expressed in CaCo2 cells, both the ~75-kDa and processed ZIP4 peptides were detected using the anti-HA antibody when zinc was deficient in the culture medium, and the abundance of the processed ZIP4 peptide relative to the full-length ZIP4 peptide increased significantly when the cells became zinc deficient. These results demonstrate that ZIP4 processing is induced by zinc deficiency. It occurs in vivo in the VYS cells and in transfected MDCK and CaCo2 cells.

The FLAG tag on the amino terminus of FLAG-ZIP4-HA allowed us to follow the fate of the ectodomain of ZIP4 in these cells. A ~35-kDa ZIP4 peptide was detected using the anti-FLAG antibody in transfected MDCK and CaCo2 cells cultured in zinc-deficient medium (Fig. 2, middle panels, and 3A and B). The approximate size of this peptide suggests that the amino-terminal domain of ZIP4 is cleaved specifically and

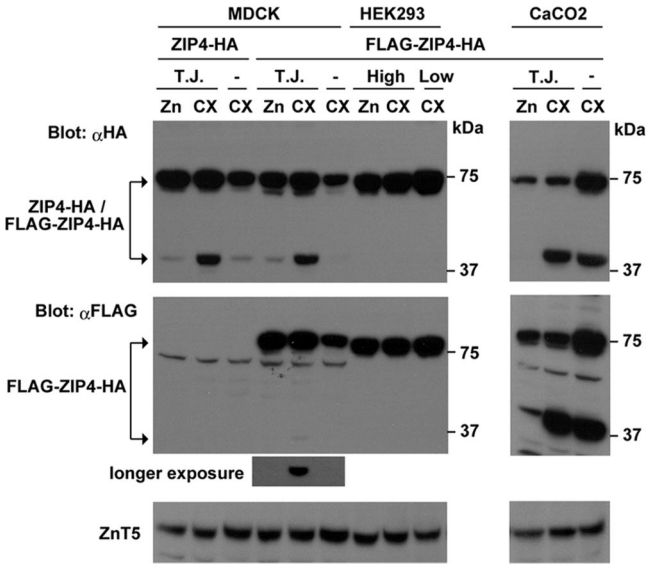

FIG. 2. ZIP4 processing in transfected MDCK and CaCo2 cells is enhanced during zinc deficiency, and the ectodomain is specifically cleaved and internalized. Pools of stably transformed MDCK cells expressing ZIP4 with a carboxyl-terminal HA tag (ZIP4-HA) or MDCK, CaCo2, and HEK293 cells expressing ZIP4 with an amino-terminal FLAG tag and a carboxyl-terminal HA tag (FLAG-ZIP4-HA) were examined (Fig. 5A). Transfected cells were cultured in medium containing 10% Chelex-treated FBS (CX) or 10% Chelex-treated FBS to which 4 μM $ZnSO_4$ was added prior to culture (Zn). Cells were examined when subconfluent (−) for 24 h in CX medium or after they formed tight junctions (TJ) when confluent for 4 days. HEK293 cells were cultured under high- or low-confluence conditions. ZIP4 was detected by Western blot analysis of total cellular proteins using an anti-HA (αHA) antibody and an anti-FLAG (αFLAG) antibody. Total cellular lysate was analyzed for CaCo2 cells (middle panel at right) using an anti-FLAG antibody which revealed a major ~35-kDa band from the amino-terminal ectodomain. A band of the same size was detected in MDCK cells after a longer exposure of the membrane. ZnT5 is shown as a loading control (lower panels).

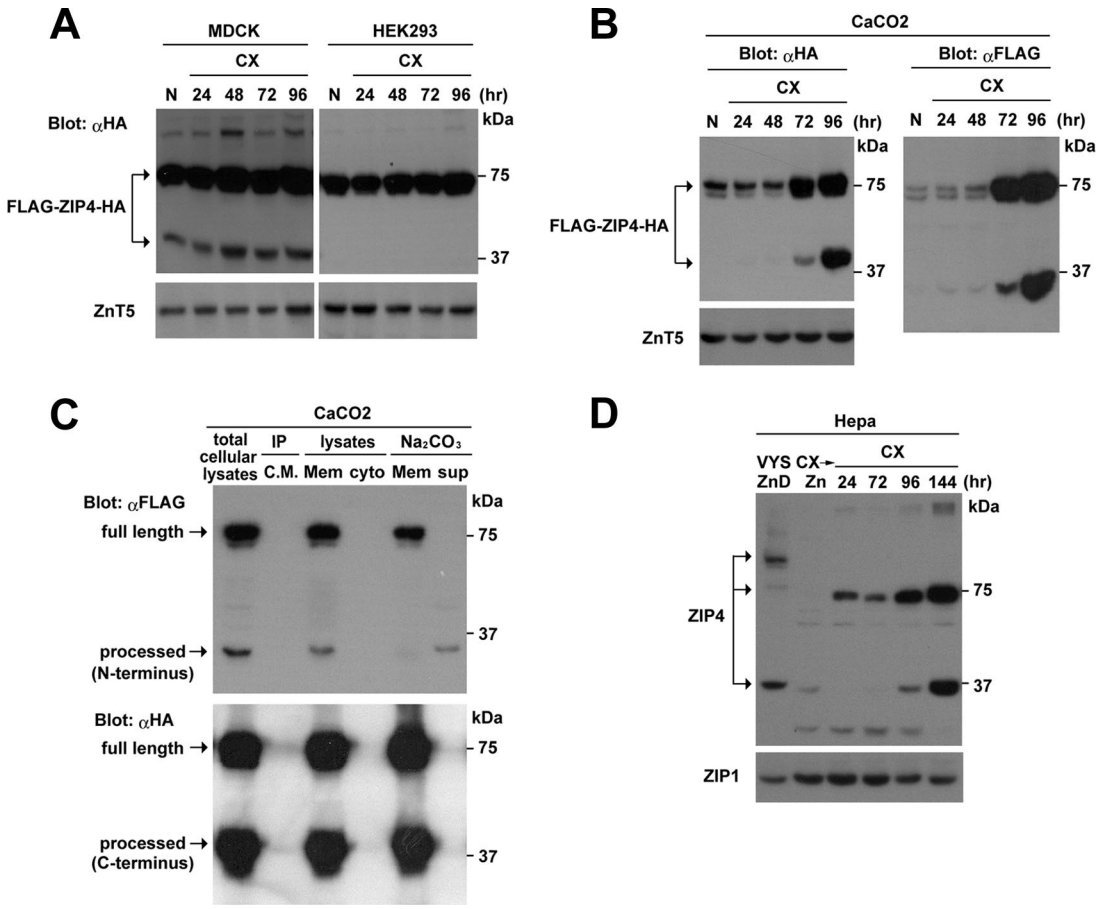

FIG. 3. ZIP4 processing is induced in zinc-deficient medium in transfected cells and in mouse Hepa cells which express the endogenous *Slc39a4* gene, and the ectodomain is loosely associated with cellular membranes. (A) Pools of stably transformed MDCK and HEK293 cells expressing FLAG-ZIP4-HA were cultured in medium containing either 10% normal FBS (N) for 24 h or 10% Chelex-treated FBS (CX) for the indicated times (24 to 96 h). MDCK cells were examined after forming tight junctions. Western blot analysis was performed using 20 μg of total cellular protein and an anti-HA antibody (αHA). ZnT5 is shown as a control. (B) Pools of stably transformed CaCo2 cells expressing FLAG-ZIP4-HA were cultured in medium containing either 10% normal FBS (N) for 24 h or 10% Chelex-treated FBS (CX) for the indicated times (24 to 96 h). Cells were examined after forming tight junctions. Western blot analysis was performed using total cellular protein (20 μg) and either an anti-HA antibody (αHA) or an anti-FLAG antibody (αFLAG). ZnT5 is shown as a control. (C) CaCo2 cells expressing FLAG-ZIP4-HA were cultured for 48 h in medium containing 10% Chelex-treated FBS, and ZIP4 was detected by Western blotting using anti-FLAG antibody (αFLAG) and anti-HA antibody (αHA). The culture medium (CM) was collected and immunoprecipitated (IP) using the anti-FLAG antibody. Membrane (Mem) and cytosolic (Cyto) fractions from these cells were prepared and subjected to Western blotting; the membrane fraction was extracted in Na_2CO_3, and the pellet and extract were also analyzed. (D) Mouse Hepa cells were cultured in medium containing 10% Chelex-treated FBS (CX) for the indicated times (24 to 144 h) or cultured for 28 h in 10% Chelex-treated FBS to which 4 μM zinc was added for the last 4 h (CX→Zn). In addition, lane 1 contains a sample of VYS membrane proteins from zinc-deficient (ZnD) pregnant mice as described in the legend of Fig. 1. Western blots were performed using membrane protein (20 μg) and an anti-peptide ZIP4 antibody directed against the intracellular loop between transmembrane domains III and IV of ZIP4 to detect endogenous ZIP4 peptides (Fig. 5). ZIP1 is shown as a control.

near the first transmembrane domain. This ectodomain peptide was detected in total cell lysates and showed a parallel response to the appearance of the processed ZIP4 peptide detected by the anti-HA antibody (Fig. 2 and 3B). In transfected CaCo2 cells the ectodomain peptide (~35 kDa) was particularly abundant in zinc-deficient cell lysates (Fig. 2, middle panels, and 3B). Long-term culture of transfected MDCK (Fig. 3A) and CaCo2 cells (Fig. 3B) in zinc-deficient medium led to increased abundance of the processed ZIP4 carboxyl-terminal peptide. The ectodomain of ZIP4 was found to be loosely associated with the membrane fraction of transfected CaCo2 cells, whereas the processed ZIP4 peptide was an integral membrane protein, as predicted. The ectodomain peptide was not detected in the cytosolic fraction from the transfected cells or in the cell culture medium after immunoprecipitation (Fig. 3C). Taken together, these results demonstrate that under conditions of zinc deficiency, ZIP4 is processed to yield a ~35-kDa amino-terminal ectodomain peptide that accumulates as a peripheral membrane protein and a ~37-kDa carboxyl-terminal processed peptide that accumulates as an integral membrane protein.

Mouse Hepa cells express and regulate the endogenous *Slc39a4* gene (33) and also process ZIP4 during long-term culture in zinc-deficient medium (Fig. 3D). After 6 days of zinc deficiency, the processed ZIP4 peptide was as abundant as the full-length ZIP4 peptide (~75 kDa) in these cells. The inclu-

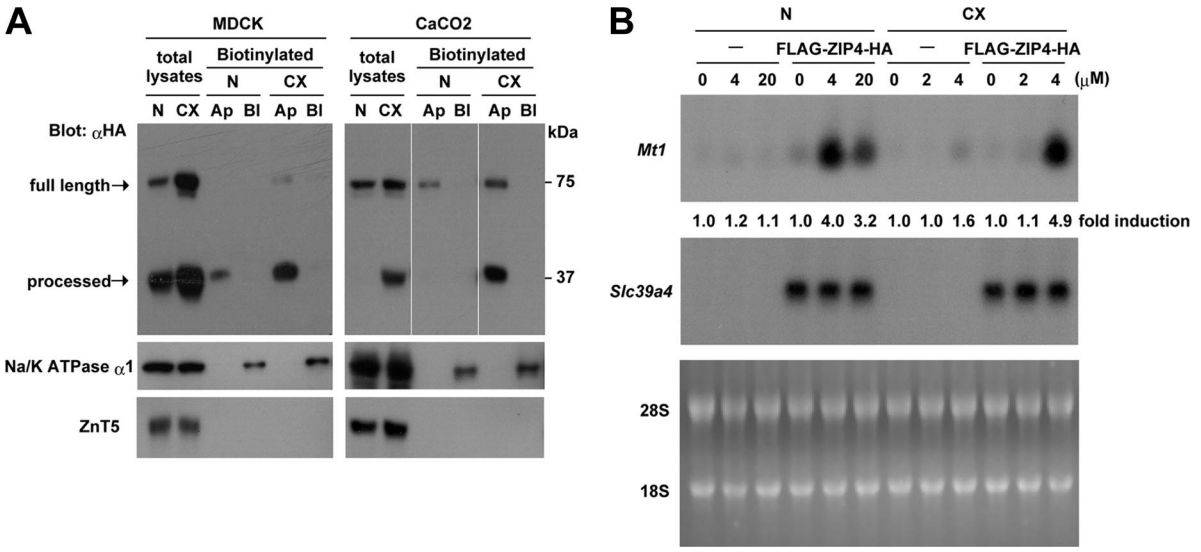

FIG. 4. The processed ZIP4 carboxyl-terminal domain preferentially accumulates in the apical membrane in MDCK and CaCo2 cells, and these cells show a dramatically decreased dose response for zinc induction of *Mt1* expression. (A) Pools of stably transfected MDCK and CaCo2 cells expressing FLAG-ZIP4-HA were grown in transwell plates until polarized and then cultured in medium containing either 10% normal FBS (N) or 10% Chelex-treated FBS (CX) for 48 h before cell surface biotinylation assays were performed. The biotinylation reagent (sulfo-NHS-SS-biotin) was added to either the apical (Ap) or basolateral (Bl) compartment of the transwell plate, as described in Materials and Methods. Solubilized proteins were captured using streptavidin beads and analyzed by Western blotting using an anti-HA antibody (αHA). Total lysates refers to aliquots of the input biotinylated proteins from the apical surface before avidin capture. The processed carboxyl-terminal peptide of ZIP4 was preferentially biotinylated in the apical membrane. ZnT5 and NaK-ATPase α1 antisera were used as controls for input and for efficiency of basolateral membrane biotinylation, respectively. (B) Nontransfected control MDCK cells (−) and pools of MDCK cells stably transfected with the FLAG-ZIP4-HA expression vector were cultured for 48 h in medium containing either 10% normal FBS (N) or 10% Chelex-treated FBS (CX). Cells were then treated from the apical chamber with the indicated concentrations of $ZnSO_4$ (0 to 20 μM) for 6 h. Total RNA (20 μg) was isolated and fractionated by formaldehyde-agarose gel electrophoresis, transferred to nylon membranes, and hybridized with mouse *Mt1* and *Slc39a4* cRNA probes. Hybrids were detected by autoradiography. Gels were stained with acridine orange as a control for RNA integrity and loading (bottom panel). The relative abundance of *Mt1* mRNA without zinc was defined as 1.0-fold induction, and the change in induction relative to that sample is shown below each lane (top panel).

sion of 4 μM zinc in the Chelex-treated 10% FBS-containing medium, which restores the normal level of zinc, completely prevented induction of ZIP4 in Hepa cells (Fig. 3D) and significantly diminished the accumulation of processed ZIP4 in transfected CaCo2 and MDCK cells (Fig. 2). Thus, the regulation of ZIP4 is extremely sensitive to zinc, and levels of zinc found in normal serum are sufficient to diminish or prevent ZIP4 accumulation.

The cell surface localization of processed ZIP4 in MDCK and CaCo2 cells expressing FLAG-ZIP4-HA was further examined using a surface biotinylation assay (Fig. 4A). Pools of stably transfected MDCK and CaCo2 cells were grown on transwell plates until polarized and then cultured for 48 h in normal or zinc-deficient medium before the addition of biotinylation reagent to the apical or basolateral compartment of the transwell and capture of the biotinylated proteins using streptavidin beads. Under these assay conditions, lysine residues exposed on the extracellular surface of the plasma membrane are biotinylated. This allowed for preferential labeling and subsequent detection of the plasma membrane-associated forms of ZIP4. Neither full-length nor processed ZIP4 was detected among the biotinylated basolateral proteins, whereas NaK-ATPase α1 subunit, a known basolateral membrane protein (34), was readily detectable. In contrast, both full-length and processed ZIP4 were detected among the biotinylated proteins from the apical membrane, and the relative abundance of the processed ZIP4 peptide in the apical membrane increased significantly during zinc deficiency (Fig. 4A). Processed ZIP4 was preferentially biotinylated in both cell types, suggesting that it is the most abundant form of ZIP4 that accumulates in the apical membrane. ZnT5, a Golgi apparatus-specific zinc transporter, was not biotinylated in these experiments. Taken together, these results reveal that processed ZIP4 is preferentially localized to the apical surface in polarized cells during zinc deficiency. This finding strengthens the concept that processed ZIP4 accumulates in the apical membrane following the removal of its ectodomain during zinc deficiency, and we infer that this process occurs in vivo based on these studies of transfected cells.

As an approach to examining the functional significance, if any, of processed ZIP4 in the plasma membrane, its potential role as a zinc transporter at the apical surface of polarized MDCK cells was monitored using the rapid induction of *Mt1* mRNA as an indirect yet physiologically relevant readout for increased intracellular zinc (11) (Fig. 4B). Basal and metal-induced transcription of mouse *Mt1* is totally dependent on the zinc-sensing transcription factor MTF-1 (6). MTF-1 directly senses increases in intracellular available zinc due to its unique zinc finger domain (13), leading to a rapid increase in the *Mt1* transcription rate. Expression of ZIP4 in transfected cells has recently been shown to cause hypersensitivity to zinc toxicity (15). Therefore, we predicted that expression of a functional

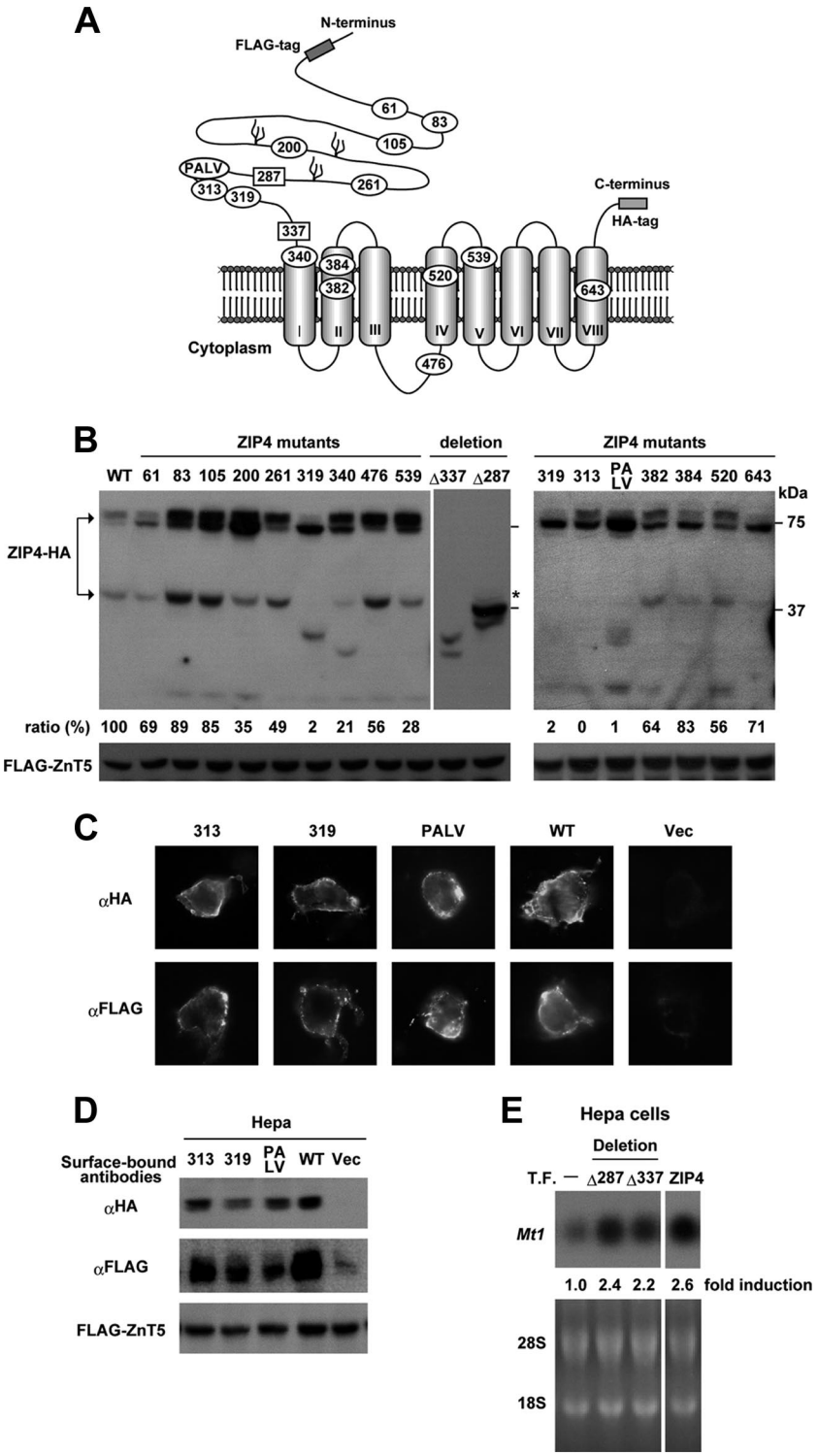

FIG. 5. During zinc deficiency, the ectodomain of ZIP4 is cleaved just before the first transmembrane domain, and cleavage is inhibited by AE mutations near a predicted metalloproteinase cleavage site motif. (A) A cartoon of the predicted membrane topology of ZIP4 is shown with eight transmembrane domains, the large extracellular ectodomain, and the large intracellular loop between transmembrane domains III and IV. The locations of FLAG and HA tags are shown, and the anti-peptide antibody against ZIP4 was raised against a peptide from the large intracellular loop. The FLAG tag was inserted just upstream of N26 in ZIP4-HA. The positions of AE mutations (10, 12, 17, 20, 32) studied in this work are indicated, as is the PALV sequence which may represent a metalloproteinase cleavage site. The extracellular localization of the ectodomain was confirmed herein as shown below in panels C and D. (B) Hepa cells were transfected with expression vectors for wild-type ZIP4-HA or the indicated ZIP4-HA mutants. The expression vector for FLAG-ZnT5 was cotransfected as a transfection control. After transfection, Hepa cells were cultured in medium containing 10% normal FBS for 24 h. The overexpression of ZIP4 in these transfection assays led to increased accumulation of processed wild-type ZIP4 in cells cultured in medium containing normal levels of zinc. Western blotting was performed using total

ZIP4 peptide would lead to a lower dose-response curve for zinc induction of *Mt1* mRNA. This was found to be the case (Fig. 4B). Control and transfected MDCK cells were cultured in medium containing normal 10% FBS or Chelex-treated 10% FBS. As shown in Fig. 4A, under these conditions processed ZIP4 was the major ZIP4 peptide biotinylated on the apical surface of these cells, and its abundance increased during zinc deficiency. The induction of *Mt1* mRNA was monitored by Northern blot hybridization 6 h after the addition of various concentrations of zinc to the culture medium from the apical side (Fig. 4B). *Mt1* mRNA induction was dramatically more sensitive to zinc in ZIP4-expressing cells than in control cells. As little as 4 μM zinc was effective at inducing this mRNA in the transfected MDCK cells cultured in normal or zinc-deficient medium, whereas 20 μM zinc was ineffective in control cells. In control cells, we noted that 100 μM zinc gave an equivalent level of induction (data not shown). This increased sensitivity to zinc was conferred due to the apical expression of ZIP4, and addition of zinc (20 μM) from the basolateral side was ineffective (data not shown). Taken together, the above results suggest that processed ZIP4 may function as a physiologically relevant zinc transporter although these results do not exclude possible contributions of unprocessed ZIP4 to the apical uptake of zinc in these transfected cells, nor do they provide information about the relative efficiency of zinc transport by processed versus unprocessed ZIP4.

Multiple mutations have been detected in the ectodomain of ZIP4 in patients with AE (Fig. 5A), but their effects on ZIP4 function are largely unexplored. Whether these AE mutations affect the accumulation of processed ZIP4 was examined (Fig. 5B) using Hepa cells transfected with the ZIP4-HA construct containing ectodomain AE mutations. The appearance of processed ZIP4 was monitored by Western blotting (Fig. 5B). When ZIP4 is overexpressed in transfected Hepa cells, a significant portion of the protein is processed and accumulates when zinc is replete. An estimate of the extent of processing was obtained by comparing the densities of the processed versus the unprocessed bands on the blot. It should be noted that two bands were detected for the full-length ZIP4-HA peptide expressed in these transfected Hepa cells. Previous studies have shown that the upper band represents glycosylated ZIP4 in transfected cells (9, 31). About half of the wild-type ZIP4 was processed under these conditions, and this value was set at 100%. As shown in Fig. 5B, among 12 AE mutations examined, two (C319Y and Q313H) profoundly diminished the accumulation of processed ZIP4, and another (G340D) significantly diminished processing. Several other mutations modestly diminished the extent of processing. The AE mutations at residues 319 and 340 sometimes lead to the appearance of smaller ZIP4 peptides from the carboxyl terminus (HA tagged), which suggests that aberrant processing can occur due to these mutations. The mutations at residues 313, 319, and 340 in ZIP4 did not prevent the accumulation of the unprocessed protein in the transfected cells, and all three are near the predicted region of cleavage of the ectodomain.

Although the precise site of ZIP4 processing is unknown, residues 319 and 313 are in close proximity to a PALV motif which resembles a metalloproteinase cleavage site (1, 30). It has been suggested previously, but not yet demonstrated, that members of the LIV-1 subfamily of ZIP proteins, to which ZIP4 belongs, have a motif that resembles the zinc-binding motif of matrix metalloproteinases (HEXPHEXGD) (27, 30). Mutating the PALV motif in ZIP4 was also found to prevent processing (Fig. 5B). The mutations at residues 313 and 319 (313 and 319 mutants, respectively) and in the PALV motif did not prevent these ZIP4 proteins from accumulating on the plasma membrane (Fig. 5C), as assessed by immunofluorescence detection of the FLAG and HA tags in fixed but nonpermeabilized cells. Detection of the FLAG epitope in this experiment is the first formal indication that the amino terminus of ZIP4 is extracellular, as was predicted. These results were confirmed by examining the amount of anti-FLAG and anti-HA antibodies that could bind to fixed and nonpermeabilized Hepa cells transfected with the FLAG-ZIP4-HA vectors (Fig. 5D). These antibodies showed minimal binding to the surface of nontransfected cells but significant binding to the surface of the transfected cells. The total amount of antibody bound was reduced, although not dramatically, for the 313, 319, and PALV mutant peptides. Although the results show that the amount of the 319 bound by the HA antibody was

cellular protein (20 μg) and an anti-HA antibody for ZIP4-HA. Most of the ZIP4 mutants used here correspond to those found in human AE patients. The numbers shown indicate the residue mutated in mouse ZIP4-HA. Mutations introduced in mouse ZIP4 were as follows (corresponding residues in the human sequence are indicated in parentheses): C61R (C62R), P83L (P84L), N105K (N106K), P200L (P200L), Q261W (R251W), C319Y (C309Y), G340D (G330D), K476A (K463A), G539R (G526R), Q313H (Q303H), L382P (L372P), G384R (G374R), H520A (H507A), and G643R (G630R). The K476 residue is a putative ubiquitination site which was mutated to alanine in the large intracellular loop. The PALV oval indicates mutation of the 308PALV311 sequence to 308ESLY311. Amino-terminal deletion mutants (Δ337 and Δ287) are indicated by the terminal amino acid remaining after the deleted portion of ZIP4. The Δ287 mutant has a deletion of residues 1 to 286, and residue 287 is methionine. The Δ337 mutant has a deletion of residues 1 to 336 just before the first transmembrane domain, and methionine was added by fusing the MEVLLGVKIGC leader peptide to the N terminus. The predicted mobility of the Δ287 mutant of ZIP4 is indicated by an asterisk. It should be noted that the 319, 313, and PALV mutants showed almost no properly processed ZIP4 peptide although smaller ZIP4 peptides were detected. An estimation of the relative efficiency of processing in each sample is shown below the top panel. FLAG-ZnT5 is shown as a control for transfection efficiency. (C) The 313, 319, and PALV mutants of ZIP4 were expressed in Hepa cells, and their localization on the cell surface was examined by immunofluorescence microscopy of fixed, nonpermeabilized cells using anti-HA (αHA) and anti-FLAG (αFLAG) antibodies. (D) The extracellular localization of the amino and carboxyl termini of the 313, 319, and PALV mutants of ZIP4 expressed in Hepa cells was examined by Western blot detection of surface-bound antibodies using a horseradish peroxidase-conjugated anti-immunoglobulin G antibody. Transfected Hepa cells were fixed and then incubated with anti-HA or anti-FLAG antibodies. After removal of unbound antibodies, the bound antibodies were solubilized and then detected by Western blotting. Vec, cells transfected with the empty vector. WT, wild type. FLAG-ZnT5 is shown as a control for transfection efficiency. (E) Hepa cells were not transfected (T.F.−) or transfected with the ZIP4-HA expression vector (ZIP4) or vectors expressing amino-terminal deletion mutants of ZIP4-HA (Δ287 and Δ337). Cells were cultured in medium containing 10% normal FBS for 24 h and then treated with $ZnSO_4$ (4 μM) for 6 h before Northern blot analysis and quantification of relative levels of *Mt1* mRNA.

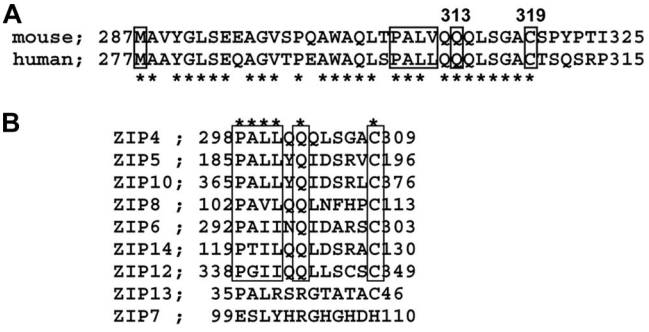

FIG. 6. Conservation of amino acids encompassing the PALV motif in human and mouse ZIP4 and conservation of this potential metalloproteinase cleavage site among several human LIV-1 subfamily members. (A) Alignment of the amino acid sequences of human and mouse ZIP4 in the region of the ectodomain near the predicted start of the first transmembrane domain. Residues we mutated in mouse ZIP4 are indicated by rectangles over the PALV, Q313, and C319 residues. Conserved amino acids are indicated by an asterisk. (B) Alignment of the amino acid sequence around a PALL motif in several human LIV-1 subfamily members. The accession numbers for the sequences used for the alignment are as follows: NP_570901 for ZIP4, NP_775867 for ZIP5, NP_065075 for ZIP10, NP_071437 for ZIP8, NP_036451 for ZIP6, NP_001121903 for ZIP14, NP_689938 for ZIP12, NP_689477 for ZIP13, and NP_008910 for ZIP7. Amino acids consistent with a putative metalloproteinase cleavage motif are boxed, and the asterisks above indicate identity or a conservative change in that amino acid within the motif.

slightly reduced in this blot, this was not confirmed using the FLAG antibody, nor did the results shown in Fig. 5B suggest a reduction in level of accumulation of the full-length mutant protein. Therefore, we conclude that these AE mutations prevent the proper processing of ZIP4 but do not significantly diminish its accumulation at the cell surface in these transfected cells.

It is interesting that a G643R mutation, which occurs in the middle of predicted transmembrane domain eight, has previously been shown to be poorly trafficked to the plasma membrane and to accumulate to high levels in the Golgi apparatus (31). This mutation prevented glycosylation of ZIP4 but did not block processing (Fig. 5B). The residue 319 and PALV mutations also apparently blocked glycosylation of ZIP4 and prevented processing. In contrast, the residue 313 mutation did not block glycosylation of ZIP4 but completely impaired processing. These results suggest that processing of ZIP4 can be independent of the glycosylation status of the protein. Processing of the G643R mutant suggests that processing can occur within the vesicular compartment.

Overall, there is relatively poor amino acid sequence conservation of the ectodomain of mouse versus human ZIP4, whereas the transmembrane domain region is well conserved (4). In the ectodomain, several blocks of amino acids are well conserved, and those amino acids, which are mutated in AE patients, are also conserved in this domain. The region around the PALV sequence, including residues 313 and 319, is highly conserved between human and mouse ZIP4 (Fig. 6A), which suggests that it may be functionally important. In addition, the sequences around similar putative metal-proteinase cleavage sites are conserved in several other members of the human LIV-1 subfamily (Fig. 6B), which suggests that processing of other ZIP proteins in this family may also occur.

To gain more insight into the identity and potential function of the processed ZIP4 peptide, we expressed ectodomain truncation mutants of ZIP4 in transfected Hepa cells and examined them by Western blotting (Fig. 5B). Expression of an amino-terminal truncation mutant of ZIP4 (deleted to residue 287) yielded a major peptide that migrated close to the apparent size of processed ZIP4, whereas truncation to residue 337 yielded smaller peptides (Fig. 5B). Transfection of Hepa cells with the amino-terminal truncation mutants of ZIP4 (deleted to residue 287 or 337) increased sensitivity to induction of *Mt1* expression by physiological concentrations (4 μM) of zinc (Fig. 5E). Taken together, these results are consistent with the concept that the ectodomain of ZIP4 is cleaved near the PALV motif and that processed ZIP4 may be physiologically important for zinc uptake.

The processing of ZIP4 and accumulation of ZIP4 peptides in the cell are dramatically enhanced by a deficiency of zinc. It has also been shown that normal or higher levels of extracellular zinc stimulate the rapid endocytosis and degradation of ZIP4 (9, 31, 33). How the processing pathway and the degradation pathway for this protein interrelate was examined (Fig. 7). Mouse Hepa cells were incubated in zinc-deficient medium to induce ZIP4 and were then treated with zinc. Restoring the normal concentration of zinc (4 μM) in the medium caused the rapid appearance of processed ZIP4 and concomitant loss of the full-length form (Fig. 7A). The processed form of ZIP4 was the most abundant form by 2 h after the repletion of zinc. However, within 6 h ZIP4 was completely degraded. These findings are consistent with the concept that very low levels of zinc initiate processing of ZIP4. When zinc concentrations are low for prolonged periods, ZIP4 processing predominates, and the processed peptides accumulate. When zinc concentrations are normal or slightly elevated, ZIP4 processing is dramatically accelerated, and the degradation pathway predominates. Previous studies have shown that zinc stimulates the endocytosis of ZIP4 (9, 15, 33). Therefore, the relationship between the endocytosis and processing of ZIP4 was examined. Two inhibitors of endocytosis (Fig. 7B) blocked the rapid processing of ZIP4 induced by the repletion of zinc in zinc-deficient Hepa cells. We also found that the dynamin inhibitors dynasore (14) and dynamin K44A (24) partially prevented the processing of ZIP4 in response to zinc repletion (data not shown). Taken together, these results suggest that ZIP4 processing involves endocytosis of the protein. Whether cleavage of the ectodomain occurs outside or inside the cell remains to be determined. However, these studies suggest that processed ZIP4 accumulates through recycling back to the plasma membrane.

The degradation of human ZIP4 in response to zinc requires endocytosis and ubiquitination of the protein, and lysine 463 in the large intracellular loop (Fig. 5A) was predicted to be the site of ubiquitination (15). In that regard we noted that mutation of lysine 476 to alanine in the large intracellular loop of mouse ZIP4 did not prevent processing (Fig. 5B). This finding suggests that the ubiquitination of ZIP4 may be responsive to zinc concentrations and may play a role in determining whether ZIP4 is processed or degraded.

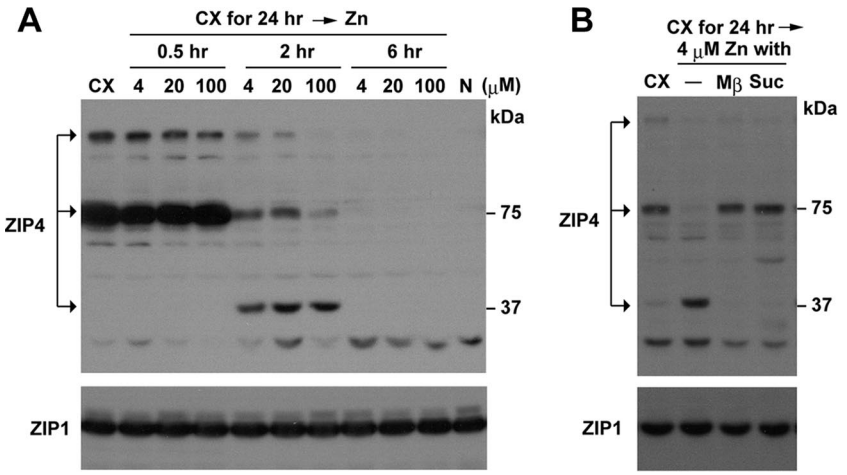

FIG. 7. The processing and degradation of ZIP4 are regulated by zinc and require endocytosis. (A) Hepa cells cultured in medium containing 10% Chelex-treated FBS (CX) for 24 h were treated with the indicated concentrations of $ZnSO_4$ (4, 20, or 100 μM) for the indicated times (0.5 to 6 h). Membrane proteins (20 μg) were analyzed by Western blotting using an anti-peptide ZIP4 antibody (top) or a ZIP1 antibody (bottom). Lane N, cells cultured in medium containing normal FBS. (B) Hepa cells were cultured in zinc-deficient medium as in panel A, treated with the indicated inhibitors for 30 min or not treated (−) and then incubated with 4 μM $ZnSO_4$ for 2 h in the presence of inhibitor. Western blotting of membrane proteins (20 μg) was performed using an anti-peptide ZIP4 antibody (top) or a ZIP1 antibody (bottom). Endocytosis inhibitors used were as follows: Mβ, 10 mM methyl-β-cyclodextrin; Suc, 350 mM sucrose.

DISCUSSION

ZIP4 is essential for proper zinc homeostasis. Mutations in this gene cause the rare human genetic disorder AE, whereas in mice this gene is essential for survival of the early embryo, and heterozygosity hypersensitizes mice to the effects of zinc deficiency (5, 10, 32). Several lines of evidence suggest that ZIP4 functions during periods of zinc deficiency, under conditions when available zinc concentrations are low. This protein is not detectable in the intestine or VYS (33) or in membrane preparations from Hepa cells (shown herein) when zinc concentrations in the diet or culture medium are normal, despite the presence of this mRNA in these cell types (4, 33). However, when zinc becomes deficient, ZIP4 protein accumulates on the apical surface of these epithelial cell types and accumulates dramatically in membranes of cultured Hepa cells. Zinc controls the localization of ZIP4 in vivo and in transfected cells (9, 15, 31). When zinc is low, more ZIP4 is synthesized and becomes localized to the cell surface; but when zinc levels return to normal, this protein is rapidly internalized and degraded. Taken together, these studies indicate that ZIP4 must have the capacity to acquire zinc from the environment very efficiently when zinc levels are very low, but it is not needed or may even be deleterious when zinc is replete. How ZIP4 accomplishes this task is unknown. The mechanism by which ZIP4 functions to facilitate zinc uptake are not well understood.

During the course of our studies of ZIP4, we found that during periods of prolonged dietary zinc deficiency a smaller ~37-kDa ZIP4 peptide accumulates to very high levels in the intestine and VYS, and by far the most prominent immunolocalization of ZIP4 is at the apical membrane of these cells (2, 33). The data presented herein establish that this ~37-kDa peptide represents ZIP4 that has undergone proteolytic processing resulting in removal of the extracellular amino-terminal ectodomain. The data obtained are consistent with the concept that ZIP4 processing requires endocytosis, which in turn suggests that processed ZIP4 is recycled back to the plasma membrane. However, further studies are required to validate that model.

It can be argued that the processing of ZIP4 may represent an intermediate step in the degradation pathway rather than representing an important part of the mechanism of action of this critical zinc transporter. A recent study of the copper transporter CTR1 revealed that the loss or absence of O-linked glycosylation leads to the proteolytic cleavage of the ectodomain and accumulation of a processed and less active transporter at the plasma membrane (16). The findings that zinc can rapidly initiate ZIP4 processing, that ZIP4 processing predominates during prolonged zinc deficiency, that processing occurs in vivo in several cell types and in several (but not all) cultured cell lines, and that it is diminished by disease-causing mutations in the ectodomain suggest that changes in O-linked glycosylation do not regulate proteolytic processing of ZIP4. Furthermore, the processing and degradation pathways for ZIP4 are apparently separable and respond differently to zinc availability. Based on these results, we infer that the processing of ZIP4 is biologically important for its function.

The evidence suggests that processed ZIP4 can function to facilitate zinc uptake when zinc concentrations are at normal levels in the culture medium. Processed ZIP4 is by far the most abundant form of the protein on the surface of transfected MDCK cells during zinc deficiency, and these cells were hypersensitive to zinc, as measured by the rapid induction of *Mt1* gene expression in response to lower and physiologically relevant concentrations of zinc in the culture medium. Furthermore, preliminary experiments suggest that Hepa cells that express forms of ZIP4 that are truncated at the amino terminus to approximate the predicted region of ectodomain cleavage also have a lower dose-response curve for zinc induction of gene expression. Although measurements of *Mt1* expression

indirectly reflect zinc transporter function, they provide a physiologically relevant reflection of rapid changes in intracellular, available zinc in cells exposed to exogenous zinc. Cells overexpressing processed ZIP4 had a dramatically lower dose-response curve for zinc induction of gene expression (Fig. 4B), and we estimated that these cells were 25-fold more sensitive to zinc than control cells (4 μM versus 100 μM, respectively) (data not shown). These experiments do not provide direct measurements of the zinc transporter activity of the processed ZIP4 peptide, but they are strongly suggestive that it may have activity. To pursue this problem in more detail will require defining the primary structure of processed ZIP4 by identifying the site(s) of ectodomain cleavage.

The ectodomain of ZIP4 must serve important functions because a large number of AE mutations are found there in human ZIP4, and the amino acids in the ectodomain that are mutated in AE patients are highly conserved between humans and mice. The identification of two AE mutations herein that block ectodomain cleavage and others that diminish it suggests that ectodomain cleavage may be important for the function of this protein in zinc homeostasis. The ectodomain of ZIP4 is internalized and can accumulate inside transfected cells, and cleavage of the ectodomain seems to be initiated by very low concentrations of zinc. These findings are intriguing and suggest the possibility that the ectodomain of ZIP4 may serve as a zinc sensor. A mutation in a conserved histidine residue in transmembrane domain IV (H520) of ZIP4 that is essential for the metal transport activities of other ZIPs (19, 23) did not block the processing of ZIP4. This finding suggests that extracellular zinc triggers processing. Although the primary sequence of the ectodomain of ZIP4 is not well conserved between humans and mice (4), in both species this domain is histidine rich (15 residues) and has several cysteine residues (6 residues). The primary sequence of the ectodomain peptide is indicative of a zinc-binding module although this has not been demonstrated. It is tempting to speculate that the ectodomain of ZIP4 functions as a high-affinity, zinc binding site that allows the chelation of zinc atoms from the environment when zinc is in very low abundance.

Ectodomain cleavage of ZIP4 is cell type specific; thus, it is not likely to be an autocatalytic process. This possibility was raised by the observation that the LIV-1 subfamily is demarcated by a highly conserved motif (HEXPHEXGD) in transmembrane domain V, which is reminiscent of a potential metalloprotease zinc-binding site (28). Members of the LIV-1 subfamily, except for ZIP7 and ZIP13, also possess a potential matrix-metalloproteinase cleavage site (in mouse ZIP4, PAL VXQXXXXXC, where X is any amino acid) near the beginning of transmembrane domain I (27, 29, 30). This sequence and these amino acids are important for the processing of ZIP4. Perhaps other LIV-1 members also undergo ectodomain cleavage and processing. It is interesting that the matrix-metalloproteinases are zinc-dependent enzymes, but our initial attempts to block matrix-metalloproteinase activity in culture did not stop ectodomain cleavage of ZIP4 during zinc deficiency (T. Kambe and G. K. Andrews, unpublished data). Whether the activity of these enzymes can be regulated by dietary zinc is unknown, as is their potential involvement, if any, in ZIP4 processing.

The concentration of zinc apparently controls a switch between the processing and accumulation versus the endocytosis and degradation of ZIP4. When zinc concentrations are low, ZIP4 undergoes ectodomain cleavage, which appears to involve endocytosis, suggesting that processed ZIP4 is recycled back to the plasma membrane. When zinc concentrations return to normal, ZIP4 undergoes rapid endocytosis and can be completely degraded. The cell can rid itself of this protein when zinc levels are normal or higher than normal. The degradation pathway in response to very high concentrations of zinc in HEK293 cells (200 μM) involves a histidine cluster in the large intracellular loop and the ubiquitination of human ZIP4, but this histidine cluster is not involved in the endocytosis of ZIP4 (15). This observation is consistent with results shown herein that these processes can be separated. Furthermore, mutation of a putative site of ubiquitination (K476) (15) in the large intracellular loop of mouse ZIP4 did not prevent ectodomain cleavage and ZIP4 processing. Endocytosis can be regulated by different modifications such as phosphorylation and sumoylation. Whether posttranslational modifications of ZIP4 are involved in ectodomain cleavage and the recycling of processed ZIP4 requires further investigation.

In summary, these studies reveal that the ectodomain of ZIP4 is cleaved and internalized during periods of zinc deficiency and that the carboxyl-terminal half of this zinc transporter accumulates on the apical surface of polarized epithelial cells, apparently reflecting recycling to the plasma membrane, where it has zinc transporter activity. AE mutations near the predicted cleavage site block ectodomain cleavage, which strongly suggests that ZIP4 processing is functionally important for proper zinc homeostasis.

ACKNOWLEDGMENTS

This work was funded, in part, by NIH grants DK063975 and DK059369 to G.K.A. T.K. was supported in part by a fellowship from the Uehara Memorial Foundation, the Naito Foundation, and the Kanae Foundation for the Promotion of Medical Science.

We thank Jim Geiser for excellent technical assistance and Benjamin P. Weaver for helpful discussions during the course of these studies.

REFERENCES

1. **Chen, E. I., S. J. Kridel, E. W. Howard, W. Li, A. Godzik, and J. W. Smith.** 2002. A unique substrate recognition profile for matrix metalloproteinase-2. J. Biol. Chem. **277:**4485–4491.
2. **Dufner-Beattie, J., Y. M. Kuo, J. Gitschier, and G. K. Andrews.** 2004. The adaptive response to dietary zinc in mice involves the differential cellular localization and zinc-regulation of the zinc transporters ZIP4 and ZIP5. J. Biol. Chem. **279:**49082–49090.
3. **Dufner-Beattie, J., S. J. Langmade, F. Wang, D. Eide, and G. K. Andrews.** 2003. Structure, function, and regulation of a subfamily of mouse zinc transporter genes. J. Biol. Chem. **278:**50142–50150.
4. **Dufner-Beattie, J., F. Wang, Y. M. Kuo, J. Gitschier, D. Eide, and G. K. Andrews.** 2003. The acrodermatitis enteropathica gene *ZIP4* encodes a tissue-specific, zinc-regulated zinc transporter in mice. J. Biol. Chem. **278:** 33474–33481.
5. **Dufner-Beattie, J., B. P. Weaver, J. Geiser, M. Bilgen, M. Larson, W. Xu, and G. K. Andrews.** 2007. The mouse acrodermatitis gene Slc39a4 (*ZIP4*) is essential for development and heterozygosity causes hypersensitivity to zinc deficiency. Hum. Mol. Genet. **16:**1391–1399.
6. **Heuchel, R., F. Radtke, O. Georgiev, G. Stark, M. Aguet, and W. Schaffner.** 1994. The transcription factor MTF-I is essential for basal and heavy metal-induced metallothionein gene expression. EMBO J. **13:**2870–2875.
7. **Kambe, T., J. Geiser, B. Lahner, D. E. Salt, and G. K. Andrews.** 2008. Slc39a1 to 3 (subfamily II) Zip genes in mice have unique cell-specific functions during adaptation to zinc deficiency. Am. J. Physiol. Regul. Integr. Comp. Physiol. **294:**R1474–R1481.
8. **Kambe, T., B. P. Weaver, and G. K. Andrews.** 2008. The genetics of essential metal homeostasis during development. Genesis **46:**214–228.

9. **Kim, B. E., F. D. Wang, J. Dufner-Beattie, G. K. Andrews, D. J. Eide, and M. J. Petris.** 2004. Zn^{2+}-stimulated endocytosis of the mZIP4 zinc transporter regulates its location at the plasma membrane. J. Biol. Chem. **279:** 4523–4530.
10. **Kury, S., B. Dreno, S. Bezieau, S. Giraudet, M. Kharfi, R. Kamoun, and J. P. Moisan.** 2002. Identification of SLC39A4, a gene involved in acrodermatitis enteropathica. Nat. Genet. **31:**239–240.
11. **Laity, J. H., and G. K. Andrews.** 2007. Understanding the mechanisms of zinc-sensing by metal-response element binding transcription factor (MTF-1). Arch. Biochem. Biophys. **463:**201–210.
12. **Lehnert, T., S. Kury, G. Burk, W. Hoepffner, and V. Schuster.** 2006. Acrodermatitis enteropathica (AE) is caused by mutations in the zinc transporter gene SLC39A4. Klin. Padiatr. **218:**221–223. (In German.)
13. **Li, Y., T. Kimura, J. H. Laity, and G. K. Andrews.** 2006. The zinc-sensing mechanism of mouse MTF-1 involves linker peptides between the zinc fingers. Mol. Cell. Biol. **26:**5580–5587.
14. **Macia, E., M. Ehrlich, R. Massol, E. Boucrot, C. Brunner, and T. Kirchhausen.** 2006. Dynasore, a cell-permeable inhibitor of dynamin. Dev. Cell **10:**839–850.
15. **Mao, X., B. E. Kim, F. Wang, D. J. Eide, and M. J. Petris.** 2007. A histidine-rich cluster mediates the ubiquitination and degradation of the human zinc transporter, hZIP4, and protects against zinc cytotoxicity. J. Biol. Chem. **282:**6992–7000.
16. **Maryon, E. B., S. A. Molloy, and J. H. Kaplan.** 2007. O-linked glycosylation at threonine 27 protects the copper transporter hCTR1 from proteolytic cleavage in mammalian cells. J. Biol. Chem. **282:**20376–20387.
17. **Meftah, S. P., H. Kuivaniemi, G. Tromp, A. Kerkeni, M. T. Sfar, A. Ayadi, and A. S. Prasad.** 2006. A new mutation in exon 3 of the SCL39A4 gene in a Tunisian family with severe acrodermatitis enteropathica. Nutrition **22:** 1067–1070.
18. **Messer, H. H., E. J. Murray, and N. K. Goebel.** 1982. Removal of trace metals from culture media and sera for in vitro deficiency studies. J. Nutr. **112:**652–657.
19. **Milon, B., Q. Wu, J. Zou, L. C. Costello, and R. B. Franklin.** 2006. Histidine residues in the region between transmembrane domains III and IV of hZip1 are required for zinc transport across the plasma membrane in PC-3 cells. Biochim. Biophys. Acta **1758:**1696–1701.
20. **Nakano, A., H. Nakano, K. Nomura, Y. Toyomaki, and K. Hanada.** 2003. Novel SLC39A4 mutations in acrodermatitis enteropathica. J. Investig. Dermatol. **120:**963–966.
21. **Peters, J. L., J. Dufner-Beattie, W. Xu, J. Geiser, B. Lahner, D. E. Salt, and G. K. Andrews.** 2007. Targeting of the mouse Slc39a2 (*Zip2*) gene reveals highly cell-specific patterns of expression, and unique functions in zinc, iron and calcium homeostasis. Genesis **45:**339–352.
22. **Prasad, A. S.** 1995. Zinc: an overview. Nutrition **11:**93–99.
23. **Rogers, E. E., D. J. Eide, and M. L. Guerinot.** 2000. Altered selectivity in an *Arabidopsis* metal transporter. Proc. Natl. Acad. Sci. USA **97:**12356–12360.
24. **Schmid, S. L., M. A. McNiven, and P. De Camilli.** 1998. Dynamin and its partners: a progress report. Curr. Opin. Cell Biol. **10:**504–512.
25. **Suzuki, T., K. Ishihara, H. Migaki, K. Ishihara, M. Nagao, Y. Yamaguchi-Iwai, and T. Kambe.** 2005. Two different zinc transport complexes of cation diffusion facilitator proteins localized in the secretory pathway operate to activate alkaline phosphatases in vertebrate cells. J. Biol. Chem. **280:**30956–30962.
26. **Tabuchi, M., T. Yoshimori, K. Yamaguchi, T. Yoshida, and F. Kishi.** 2000. Human NRAMP2/DMT1, which mediates iron transport across endosomal membranes, is localized to late endosomes and lysosomes in HEp-2 cells. J. Biol. Chem. **275:**22220–22228.
27. **Taylor, K. M., H. E. Morgan, A. Johnson, L. J. Hadley, and R. I. Nicholson.** 2003. Structure-function analysis of LIV-1, the breast cancer-associated protein that belongs to a new subfamily of zinc transporters. Biochem. J. **375:** 51–59.
28. **Taylor, K. M., H. E. Morgan, A. Johnson, and R. I. Nicholson.** 2004. Structure-function analysis of HKE4, a member of the new LIV-1 subfamily of zinc transporters. Biochem. J. **377:**131–139.
29. **Taylor, K. M., H. E. Morgan, A. Johnson, and R. I. Nicholson.** 2005. Structure-function analysis of a novel member of the LIV-1 subfamily of zinc transporters, ZIP14. FEBS Lett. **579:**427–432.
30. **Taylor, K. M., and R. I. Nicholson.** 2003. The LZT proteins; the LIV-1 subfamily of zinc transporters. Biochim. Biophys. Acta **1611:**16–30.
31. **Wang, F. D., B. E. Kim, J. Dufner-Beattie, M. J. Petris, G. Andrews, and D. J. Eide.** 2004. Acrodermatitis enteropathica mutations affect transport activity, localization and zinc-responsive trafficking of the mouse ZIP4 zinc transporter. Hum. Mol. Genet. **13:**563–571.
32. **Wang, K., B. Zhou, Y. M. Kuo, J. Zemansky, and J. Gitschier.** 2002. A novel member of a zinc transporter family is defective in acrodermatitis enteropathica. Am. J. Hum. Genet. **71:**66–73.
33. **Weaver, B. P., J. Dufner-Beattie, T. Kambe, and G. K. Andrews.** 2007. Novel zinc-responsive posttranscriptional mechanisms reciprocally regulate expression of the mouse Slc39a4 and Slc39a5 zinc transporters (Zip4 and Zip5). Biol. Chem. **388:**1301–1312.
34. **Zimnicka, A. M., E. B. Maryon, and J. H. Kaplan.** 2007. Human copper transporter hCTR1 mediates basolateral uptake of copper into enterocytes: Implications for copper homeostasis. J. Biol. Chem. **282:**26471–26480.